Journal of Magnetic Resonance 209 (2011) 149–155

Contents lists available at ScienceDirect

Journal of Magnetic Resonance

journal homepage: www.elsevier.com/locate/jmr

o-Semiquinonato and o-iminosemiquinonato rhodium complexes. EPR study of the reactions in coordination sphere of rhodium

M.P. Bubnov, I.A. Teplova, K.A. Kozhanov *, G.A. Abakumov, V.K. Cherkasov

G.A. Razuvaev Institute of Organometallic chemistry of Russian Academy of Sciences, 49 Tropinina str., Nizhny Novgorod 603950, Russia

ARTICLE INFO

Article history:
Received 20 October 2010
Revised 21 December 2010
Available online 14 January 2011

Keywords:
Rhodium
O-ligands
EPR spectroscopy
Structure elucidation

ABSTRACT

The number of dicarbonyl-o-semiquinonato (o-iminosemiquinonato) rhodium complexes was isolated and characterized. Some reactions of these compounds with tertiary phosphines (substitution, addition) were studied by EPR in solution using o-semiquinones (o-iminosemiquinones) as spin labels.

1. Results and discussion

o-Semiquinones and o-iminosemiquinones were successfully used as spin labels for investigation of reactions [1,2] and dynamic processes [3,4] occurring in the coordination sphere of metals. One of the mostly interesting our papers was dedicated to carbonyl-o-semiquinonato complexes of rhodium [2]. In some cases the nature of o-semiquinone used as spin label has some significance [4]. Analogously to previously reported [2] we have used the number of quinones – the derivatives of 3,6-di-tert-butyl-o-benzoquinone and o-iminoquinone for synthesis of new dicarbonyl rhodium(I) complexes. Then we have studied some reactions occurring in the coordination sphere of the complexes by EPR. It should be noted at the very beginning that we discuss here only the unambiguously interpreted EPR spectra.

The exchange reaction of o-semiquinonato thallium with (dicarbonyl)(chloro)rhodium(I) was used for complexes synthesis:

$$1/2[(CO)_2RhCl]_2 + TlSQ \rightarrow (CO)_2Rh(SQ) + TlCl$$

Synthetic procedure and complexes numbering for dicarbonyl rhodium o-semiquinonates **1–6**.

All the compounds were isolated and characterized by IR and EPR spectroscopy. IR spectra of all complexes contain two intensive bands C≡O stretch vibrations. NIR spectrum is characterized by at least one band of electron transfer in the region 1200–1700 nm.

High intensity of bands in the region 1450 cm^{-1} attributed to stretch vibrations of CO – sesquialteral bond evidences the anion-radical coordination mode of the ligand. Presence of the broad band in NIR area which is attributed to charge transfer from generalized d_z^2-orbital in the molecular stack to π^*_{SQ}-orbital of the ligand in the complex $(CO)_2Rh$(3,6-DBSQ) (1550 nm) [5] confirm the similar structure of all compounds.

EPR spectra of complexes **1–6** confirm the conclusion about the anion-radical coordination mode of the ligand; the charge distribution is $(CO)_2Rh^{+1}SQ^{-\cdot}$. *g*-Factor magnitudes (Table 1) are close to that typical for free unpaired electron value 2.0023. Hyperfine structure reflects only splitting with magnetic nuclei of semiquinonato ligand. We have never observed the splitting with rhodium nuclear (^{103}Rh, $I = 1/2$, 100%).

SQ = 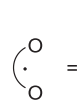 =

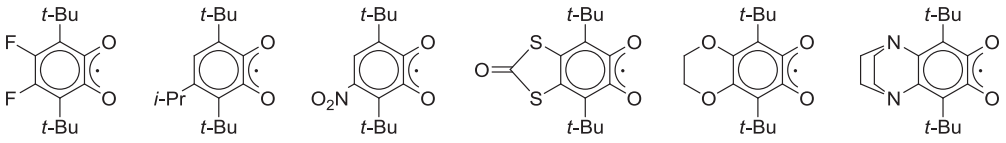

Complex: **1** **2** **3** **4** **5** **6**

(1)

* Corresponding author. Fax: +7 831 4627497.
E-mail address: kostik@iomc.ras.ru (K.A. Kozhanov).

1090-7807/$ - see front matter © 2011 Elsevier Inc. All rights reserved.
doi:10.1016/j.jmr.2011.01.002

Table 1
Frequencies of C≡O stretch vibrations in IR, electron transfer bands in NIR spectra and g_i – factors for complexes **1**–**6**.

Complex	1	2	3	4	5	6
ν (C≡O), cm^{-1}	2068	2066	2065	2075	2073	2055
	2018	2010	1997	2005	2004	2015
ν ($d_Z^2 \rightarrow \pi_{*SQ}$), cm^{-1}	7200	6200	~10,000	~8000	~10,000	6500
g_i	2.0032	2.0026	2.0025	2.0043	2.0026	2.0023

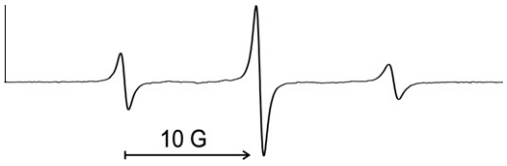

Fig. 1. EPR spectrum of complex **1** (ambient temperature, toluene).

EPR spectrum of **1** in solution is triplet (Fig. 1) due to hyperfine splitting on two equivalent fluorine nuclei (^{19}F, $I = 1/2$, 100%), $a_{iso}(F_1) = a_{iso}(F_2) = 10.8$ G. Peak intensities ratio of presented EPR spectrum (toluene, ambient temperature) differs from theoretical 1:2:1 because of different line widths of individual components ($\Gamma_1 = 0.6$ G, $\Gamma_2 = 0.52$ G, $\Gamma_3 = 0.78$ G; Γ – line width). This line broadening is caused by anisotropy of hyperfine splitting on ^{19}F nuclei and was observed earlier [6].

EPR spectrum of **2** in solution is doublet of multiplets (Fig. 2). Hyperfine structure results from interaction of unpaired electron with proton of semiquinonic ring $a_i(H(SQ)) = 3.80$ G, –CH– proton of *iso*-propyl $a_i(H(C\text{-}H)) = 0.26$ G and methyl protons of *iso*-propyl $a_i(6H(2CH_3)) = 0.53$ G. Individual components in doublet are not resolved because of lines widths are close to hyperfine coupling constants. Exact splitting constants were obtained by simulation in "WINEPR SimFonia" Version 1.25. Simulated spectrum is presented together with experimental one in Fig. 2a.

EPR spectrum of **3** is doublet of triplets (1:1:1) (Fig. 2b). Hyperfine structure is caused by interaction of unpaired electron with back-bonded proton of semiquinone ring $a_i(H(SQ)) = 3.00$ G and nitrogen nucleus of $-NO_2-$group $a_i(N) = 0.71$ G (^{14}N, I = 1, 99.63%).

EPR spectrum of **4** is singlet because of the absence of the magnetic nuclei in its structure. Due to narrow line we were able to observe satellites – hyperfine structure on two magnetic nuclei ^{13}C (I = 1/2, 1.11%) of semiquinonato carbonyl groups $a_i(2^{13}C) = 2.35$ G.

EPR spectrum of **5** – quintet (1:4:6:4:1) with satellites (Fig. 3a). It is the consequence of splitting on four equivalent protons of glycol cycle $a_i(4H) = 0.59$ G and two ^{13}C, $a_i(2^{13}C) = 2.71$ G. It should be mentioned that all four protons of glycol cycle are equivalent at all examined temperature range (180–300 K). It means that inversion of glycol cycle is fast according to EPR time scale in this temperature range (Scheme 1).

EPR spectrum of **6** can be well resolved only at low temperature in much diluted solution. The complicated multiplet (Fig. 3b) is caused by interaction of unpaired electron with two nitrogen nuclei $a_i(2N) = 0.35$ G and four protons of piperazine bicycle $a_i(4H) = 1.10$ G. Hyperfine coupling constants were obtained by simulation as well. Observable splitting only on four methylene protons of eight ones is caused by rigid configuration of piperazine substituent in contrast to previously described glycol one [7].

Scheme 2 represents the spatial configuration of piperazine substituent as a result of molecular modeling ("HyperChem" 8.0.3). It is in agreement with structural results which are known for the catecholate dianion of this o-quinone [8]. It becomes clear that four protons (H*) can effectively interact with orbital occupied by unpaired electron which is π^* in character.

o-Iminosemiquinonato complex **7** was synthesized similarly to o-semiquinonato ones. It was isolated and characterized by NIR-IR and EPR spectroscopies.

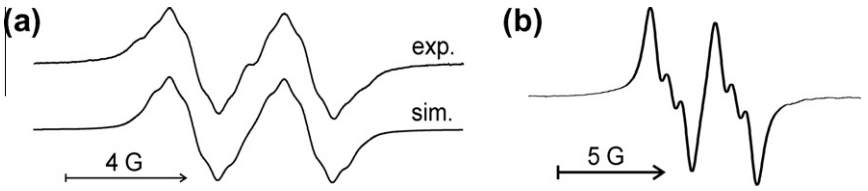

Fig. 2. EPR spectra of complexes: a – complex **2**, top: experimental (ambient temperature, toluene), bottom: its simulation; b – complex **3** (240 K, toluene).

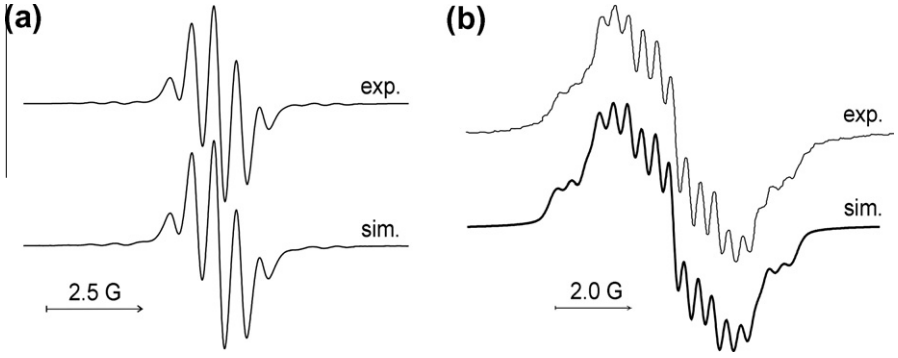

Fig. 3. EPR spectra of complexes: a – complex **5** (300 K, toluene) and its simulation; b – complex **6** (230 K, toluene) and its simulation.

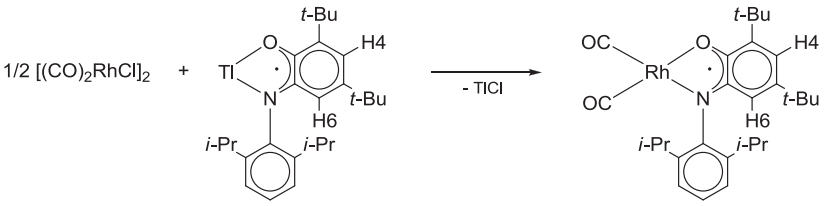

(2)

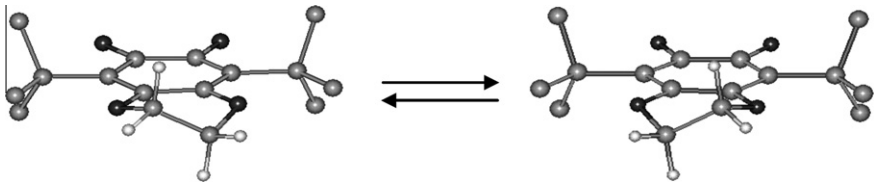

Scheme 1. Inversion of glycol cycle of semiquinone in complex **5**.

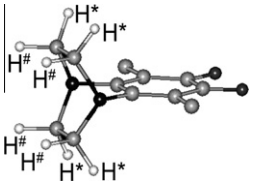

Scheme 2. Spatial configuration of piperazine substituent in semiquinone of 6 (methyl groups of tert-butyls are omitted for clarity).

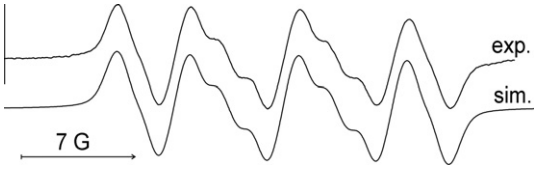

Fig. 4. EPR spectrum of **7** (300 K, toluene) and its simulation.

Synthetic procedure for dicarbonyl rhodium o-iminosemiquinonate complex 7.

IR spectrum of **7** contains two intensive bands of bond stretch vibrations C≡O (2070 and 2020 cm^{-1}). Electron transition in NIR is about 9300 cm^{-1}. EPR spectrum of **7** (Fig. 4) is triplet (1:1:1) of doublets (g_i = 2.0021) with broad lines (Γ = 1.2 G). It reflects hyperfine coupling with nitrogen nucleus a_i(N) = 6.85 G; ring protons: H4 a_i(H4) = 4.50 G and H6 a_i(H_6) = 1.35 G. Lines widths are essentially larger than that in semiquinonato analogs; it is typical for iminosemiquinones [9]. For complete simulation it is necessary to take into account the splitting constants on nine protons of *tert*-butyl in 5-position (~0.3 ΓG). This hyperfine structure is not resolved but the presence of this splitting creates the required line shape.

All synthesized compounds interact with mono- and bidentate tertiary phosphines. Composition and structure of products were established by EPR in solution.

Complexes **2**, **4**, **5**, **6** and **7** attach one molecule of triphenylphosphine eliminating one molecule of carbon monoxide and form four-coordinate square-planar complexes. Their EPR spectra parameters are listed in Table 2.

Table 2
EPR spectral parameters of four-coordinate phosphino-carbonyl rhodium adducts.

Adduct	g_i	a_i(^{31}P), G	a_i (nuclei of substituents in SQ-ring), G
2 + PPh_3	2.0052	3.60	3.40 (1H)
4 + PPh_3	2.0062	3.40	No magnetic nuclei
5 + PPh_3	2.0047	2.52	Hyperfine coupling constants
6 + PPh_3	2.0050	3.80	are less than line width
7 + PPh_3	2.0079	7.95	7.80 (N); 4.30 (H4); 1.40 (H6)

Substitution reaction of dicarbonyl-semiquinonato-rhodium with triphenylphosphine.

In the cases of complexes **2**, **4** and **6** the addition of excess of triphenylphosphine leads to five-coordinate adducts which geometry is close to trigonal bipyramid with phosphorus atoms in axial positions. It follows from large values of splitting constants on phosphorous nuclei (15.6–17.4 G) (Table 3) in contrast to 2.52–3.80 G typical for phosphorus in planar position [2].

The reaction of addition of the second triphenylphosphine molecule is reversible. Analogous phenomenon for $(CO)_2$Rh(3,6-DBSQ) was already described [2]. In the cases of other complexes (**5** and **7**) the binding of the second phosphine molecule do not occur even at large excess of PPh_3.

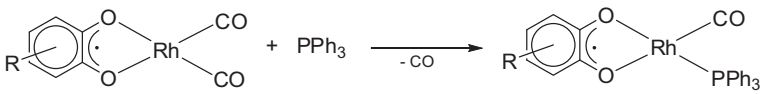

(3)

Table 3
EPR spectral parameters of di-phosphine adducts of complexes **2**, **4** and **6**.

Adduct	g_i	$a_i(^{31}P)$, ΓG	$a_i(H)$, ΓG
2 + 2 PPh_3	2.0006	17.0	3.4 (1H)
4 + 2 PPh_3	2.0016	15.6	No protons
6 + 2 PPh_3	2.0013	17.4	Line width is larger than splitting constant

The thermodynamic parameters of the reversible binding of the second phosphine molecule to mono-phosphine adducts of complexes **2** and **6** were determined. For example in the case of **2** in toluene in the presence of 100-fold excess of phosphine one can observe mono-phosphine adduct "**a**" at the temperature above ~300 K in EPR spectrum and di-phosphine adduct "**b**" at the temperature below ~200 K (Fig. 5). At intermediate temperature one can observe superposition of both spectra. EPR spectral parameters of both adducts were determined. Both spectra were simulated and summarized in different ratio in order to simulate the experimental spectra at different temperatures. Spectral intensities (double integrated) ratio and known triphenylphosphine concentration ($[PPh_3] = 10^{-2}$ mole/l) allowed to calculate the equilibrium constants at different temperatures.

$$K_P = \frac{[b]}{[a] \times [PPh_3]}$$

$$\ln K_p = -\Delta G^o/RT = -\Delta H^o/RT + \Delta S^o/R$$

Using the dependence $\ln K_p$ – 1/T allowed to estimate thermodynamic parameters of equilibrium: for **2** $\Delta H^o = -27 \pm 3$ kJ/mole, $\Delta S^o = -73 \pm 8$ J/K mole; for **6** $\Delta H^o = -22.4 \pm 2.5$ kJ/mole, $\Delta S^o = -29.3 \pm 2.0$ J/K mole. The same sign of enthalpy and entropy means that these factors act on the equilibrium position in opposite directions. Enthalpy stabilizes five-coordinated product "**b**" which has more bonds, whereas entropy favorable is four-coordinated complex "**a**" which is formed due to dissociation.

Complex **1** interacts with triphenylphosphine too. But the EPR spectral picture which is observed at different temperatures is too complicated because of inhomogeneously broadening of lines due to anisotropy of hyperfine coupling with fluorine nuclei, because of superposition of two spectra of adducts with one and two triphenylphosphine ligands and moreover spectrum of adduct with one phosphine molecule has different splitting constants on fluorine nuclei. Fig. 6 presents temperature dependence of EPR spectrum of complex **1** with excess of PPh_3. Hyperfine coupling constants on fluorine, phosphorus and rhodium nuclei in di-phosphine adduct were estimated with the help of the simulation: $g_i = 2.0013$, $a_i(2P) \cong 16.1$ G; $a_i(2F) \cong 8.9$ G; $a_i(Rh) \cong 1.3$ G.

Sterical hindrances of neutral ligand play the key role in the formation of the coordination sphere. Using of the more sterically bulky tri-o-tolyl-phosphine instead of triphenylphosphine in reaction with complexes **1**, **2** and **6** results in forming of four-coordinate adducts. Their EPR spectra parameters are listed in Table 4. The excess of the ligand do not lead to di-phosphine products.

$$(CO)_2Rh(SQ) + o\text{-}Tol_3P \rightarrow (CO)(o\text{-}Tol_3P)Rh(SQ) + CO$$

Adduct of **1** with o-Tol_3P has configuration close to square-planar. It is confirmed by different splitting constants on fluorine nuclei occupying 4 and 5 positions of semiquinone. It is the consequence of different trans-effects of carbonyl C≡O and o-Tol_3P ligands both situated in the plane of the complex. The anisotropy of hyperfine coupling with fluorine nuclei is observed in the EPR spectrum of phosphine adduct as well as in parental complex (Fig. 7).

The reactions with bidentate phosphine ligands are presented selectively because in most cases resulting EPR spectra cannot be interpreted unambiguously. Therefore, the most understandable spectra are generated in the reactions of complex **4** because of the absence of magnetic nuclei in its semiquinone.

Bidentate P-donors dppe, dppph and dppbiphen interact with **4** forming five-coordinate products where one phosphorus occupy axial and the other one – planar positions relatively to semiquinone plane.

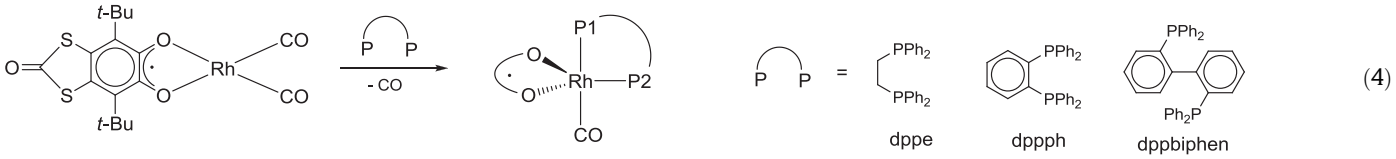

(4)

Interaction of dicarbonyl-semiquinonato-rhodium complex **4** with di-phosphines.

Different positions of phosphorus atoms follow from different HFC constants (Table 5). Using of previous experience [1–4] allow us to attribute each splitting constant to corresponding phosphorus. Phosphorus laying in the plane (P2) usually has splitting constant value about 2.0–4.0 G. Splitting constant on the phosphorus situated in axial position (P1) depends on the nature of ligand being in trans-position to it. HFC constant 5.0–5.6 G is too small for axial position comparing with similar values in trigonal-bipyramidal adducts of PPh_3 which were discussed above (15.6–17.4 G). It can be explained by the properties of ligand situated in trans-position. It is C≡O – the ligand which is strong π-acceptor in contrast to PPh_3. The same situation was already observed [2]: appearing of C≡O – ligand in trans-position to arsenic diminished splitting constant from 17.0 to 8.6 G.

The EPR spectrum of reaction mixture of complex **5** and dppbiphen is doublet of triplets of multiplets: $g_i = 2.0012$, $a_i(P) = 7.53$ G, $a_i(P/Rh) \cong 1.8/1.65$ G, $a_i(4H) \cong 0.59$ G. Only two coupling constants can be unambiguously attributed: $a_i(P) = 7.53$ G and $a_i(4H) \cong 0.59$ G. Coupling constants 1.8 and 1.65 G are close one to another and it is impossible to attribute each of them to rhodium or to the second phosphorus. Different coupling constants on the phosphorous atoms indicate their different positions: one occupies planar position and the other one – axial.

Iminosemiquinonato complex **7** interacts with mono- and di-phosphines. Reaction with PPh_3 results in square-planar four-coordinate compound. In the case of bidentate bis-(diphenylphosphino)ferrocene (dppfc) only one of PPh_2-groups is able to coordinate. It is well illustrated by the similarity of EPR spectra of PPh_3 and dppfc – adducts (Fig. 8 and Table 6). In spite of splitting constant a_i(H6) in iminosemiquinone is less than linewidth (Γ), it

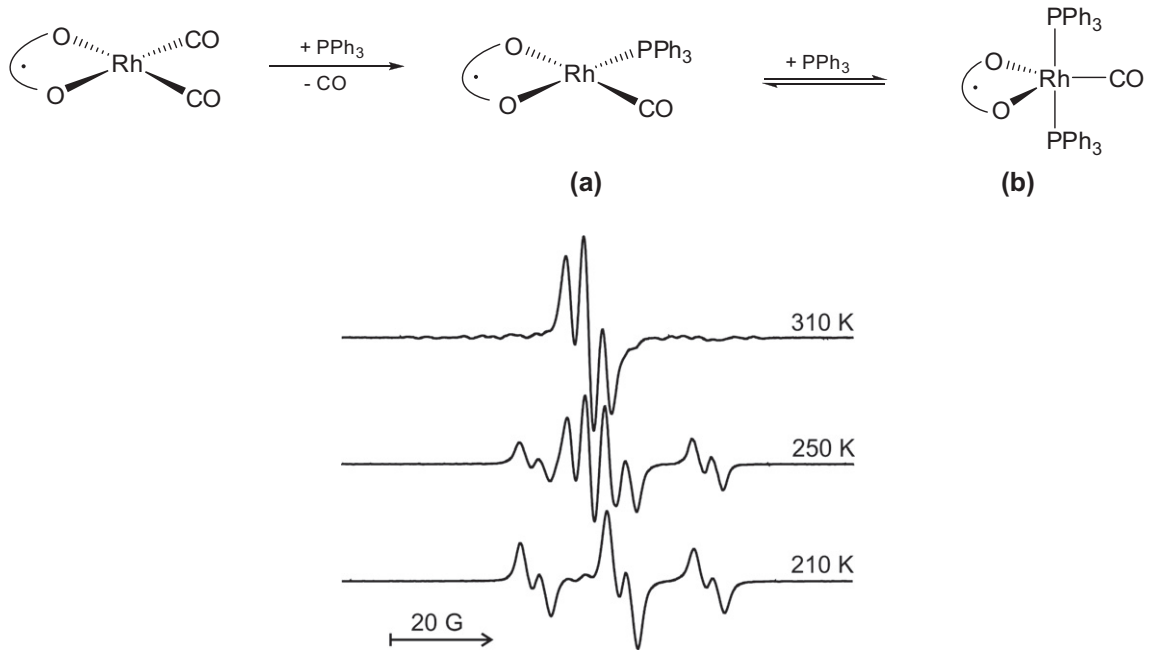

Fig. 5. Reaction scheme and EPR spectrum of reaction mixture of complex **2** and excess of PPh_3 at different temperatures. One can observe virtually individual spectra of four-coordinate adduct "a" at 310 K and adduct "b" at 210 K.

should taken into account in order to simulate the EPR spectrum sufficiently.

It is difficult to interpret exactly the geometry of adducts because large (compared to similar o-semiquinonato adducts) splitting constant with phosphorous nucleus can be the result of tetrahedral distortion (due to bulky substituent at nitrogen) as well as larger spin density transfer from iminosemiquinone to metal and phosphine ligands. In general splitting constants are close to that which were observed for similar iminosemiquinonato nickel compounds [9].

The most interesting situation one can observe in the case of interaction of complex **7** with dppbiphen. EPR spectrum contains superposition of spectra of two products converting one to another. The first spectrum (**7a**) indicates one PPh_2 group and it is similar to previously discussed: $g_i = 2.0079$, $a_i(P) = 8.0$ G, $a_i(N) = 7.8$ G, $a_i(H4) = 4.2$ G, $a_i(H6) = 1.7$ G, $\Gamma = 3.7$ G. The second spectrum (**7b**) is the doublet of doublets of multiplets: $g_i = 2.0250$, $a_i(P1) = 160.0$ G, $a_i(P2) = 26.0$ G, $a_i(N) = 7.0$ G, $a_i(H4) = 4.0$ G, $\Gamma = 8.5$ G (Fig. 9). According to EPR data one of the phosphorus occupies planar position and the other one is situated in axial site. The larger value of g-factor, very large splitting constants with both phosphorous nuclei and relatively small coupling constants with the iminosemiquinone's nuclei indicate relatively large spin density transfer from iminosemiquinonato ligand towards metal fragment. Temperature variation results in reversible

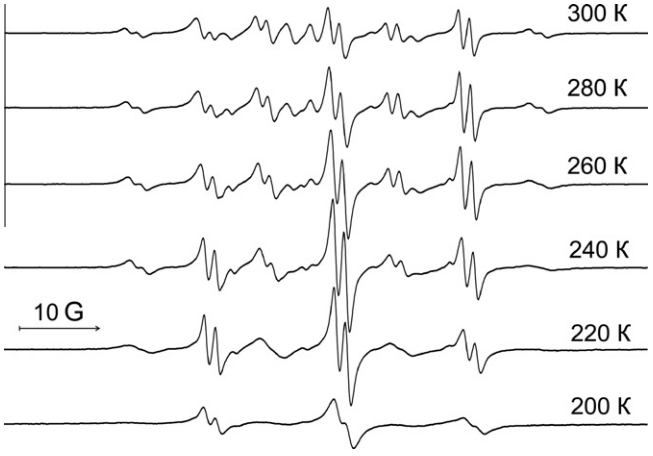

Fig. 6. Temperature dependence of EPR spectrum of reaction mixture of complex **1** with excess of PPh_3.

change of spectral intensities. When the temperature grows up intensity of spectrum **7b** decreases whereas **7a** intensity increases. This is typical for slow (in EPR time scale) interconversion of two products (Eq. (5)).

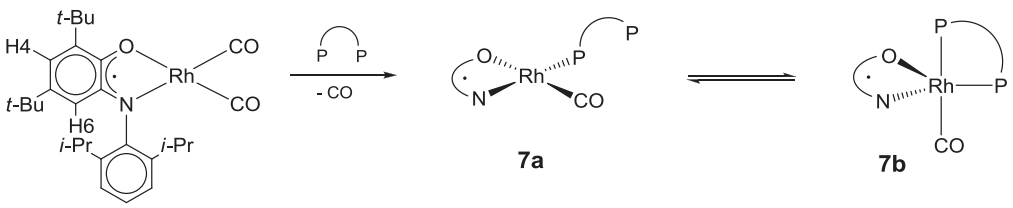

(5)

Table 4
EPR spectral parameters of adducts of complexes **1**, **2** and **6** with o-Tol$_3$P.

Adduct	g_i	a_i(P), G	a_i(H), G	a_i(F), G
1 + o-Tol$_3$P	2.0065	3.25	–	8.80/11.10
2 + o-Tol$_3$P	2.0054	3.35	3.35	–
6 + o-Tol$_3$P	2.0018	3.60	HFC constants are less than lines width	

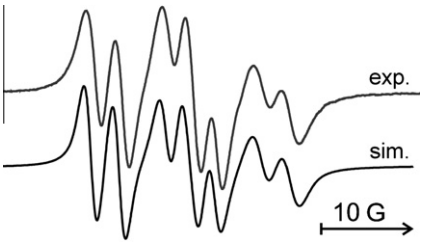

Fig. 7. Experimental EPR spectrum for adduct of **1** with o-Tol$_3$P (ambient temperature, toluene) view (top) and its simulation (bottom).

Table 5
EPR spectral parameters of products of interaction of complex **4** with different di-phosphines.

Ligand	g_i	a_i(P1), G	a_i(P2), G	a_i(Rh), G
dppe	2.0018	5.00	2.20	1.35
dppph	2.0021	5.60	2.20	1.38
dppbiphen	2.0030	5.20	2.35	1.45

Interaction of dicarbonyl-iminosemiquinonato-rhodium with dppbiphen.

2. Conclusion

Dicarbonyl-o-semiquinonato rhodium complexes have similar structures in spite of different semiquinonato ligands. EPR spectra reflect splitting on the magnetic nuclei of semiquinone. As it was demonstrated earlier [2] the mentioned compounds interact with tertiary phosphines forming square-planar phosphine-carbonyl species. Some of species attach additional molecule of PPh_3 forming five-coordinate adducts which geometry is close to trigonal bipyramid. In the case of bidentate phosphines three products which were unambiguously interpreted by EPR have one phosphorous function in the axial position and the other one in the plane of semiquinonato ligand.

An EPR spectrum of dicarbonyl-o-iminosemiquinonato complex reflects splitting on nitrogen and two protons; line width is larger than that in the most semiquinonato species. The HFC constants of phosphine products are in general larger than that in corresponding semiquinonato species. Interaction of dicarbonyl-o-iminosemiquinonato complex with 1,1′-bis(diphenylphosphino)-diphenyl leads to forming of two products: four-coordinated with singly connected di-phosphine and five-coordinated with doubly connected di-phosphine. The last product has one axial and the other planar situated PPh_2-groups. Splitting constant with axial phosphorous nucleus has extremely large value 160 G.

Table 6
EPR spectral parameters of adducts of complex **7** with PPh3 и dppfc.

Adduct	g_i	a_i(P), G	a_i(N), G	a_i(H4), G	a_i(H6), G	Γ, G
7 + PPh_3	2.0079	7.95	7.80	4.30	1.40	3.2
7 + dppfc	2.0079	7.90	7.80	4.40	1.70	3.5

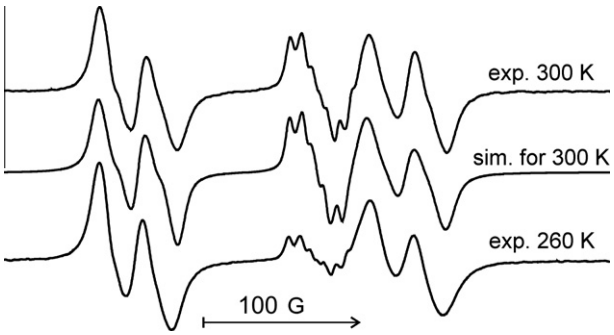

Fig. 9. Superposition of EPR spectra of **7a** and **7b** at two temperatures and it simulation for 300 K.

3. Experimental

EPR spectra were recorded on X-band spectrometers "Bruker ER 200D-SRC" and "Bruker EMX". IR-NIR spectra were registered on Fourier spectrometers "Bruker VERTEX 70" and "FSM 1201". Solvents were purified according known procedures [10]. $[(CO)_2RhCl]_2$ was obtained according to [11]. o-Quinones and o-iminoquinone were obtained according to literature procedures: **1**-[6], **2**-[12], **3**-[13], **4**-[14], **5**-[15]], **6**-[7], **7**-[16]. All the operations with o-semiquinonato (o-iminosemiquinonato) derivatives were carried out in evacuated ampoules.

4. Synthesis of dicarbonyl-o-semiquinonato-rhodium complexes

4.1. General procedure

THF solution (30 ml) of corresponding quinone (0.5 mmole) was shaken with thallium amalgam (~40% wt. of Tl, large excess) (in the case of **5** sodium dispersion was used instead of thallium amalgam) until the colour becomes unchanged. Resulting solution was decanted from amalgam into the other ampoule containing 0.5 mmole of the same quinone. The solvent was changed to toluene and the solution was used "in situ". o-Iminosemiquinonato thallium was obtained according to [17].

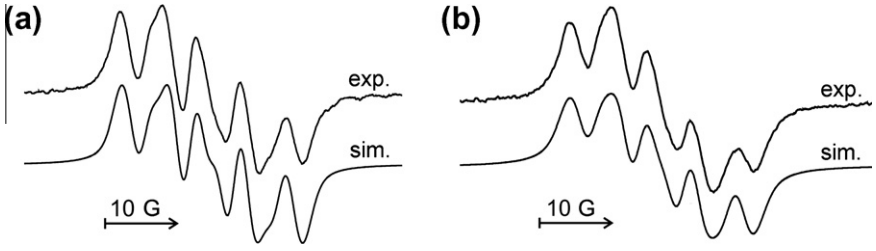

Fig. 8. EPR spectra of adducts of complex **7** with PPh_3 (a) and dppfc (b) and their simulations.

Solution of semiquinonato-thallium (sodium for **5**) was added to $[(CO)_2RhCl]_2$ (0.194 g, 0.5 mmole). Reaction mixture was warmed (60 °C) during 30–60 min and then filtered. Solvent was changed to *n*-hexane (in the case of **7** acetonitrile). Resulting solution was allowed to stay at −18 °C overnight. Microcrystalline powder was isolated by filtration.

Dicarbonyl(4,5-di-fluoro-3,6-di-tert-butyl-o-benzosemiquinonato)rhodium (**1**).

Yield: ~50%. Analysis. Founded (%): C 46.37, H 4.54, Rh 24.67. Calculated for $C_{16}H_{18}F_2O_4Rh$: C 46.28, H 4.37, Rh 24.78.

Dicarbonyl(4-iso-propyl-3,6-di-tert-butyl-o-benzosemiquinonato)rhodium (**2**).

Yield: ~30%. Analysis. Founded (%): C 53.98, H 6.13, Rh 24.28. Calculated for $C_{19}H_{26}O_4Rh$: C 54.16, H 6.22, Rh 24.42.

Dicarbonyl(4-nitro-3,6-di-tert-butyl-o-benzosemiquinonato)rhodium (**3**).

Yield: ~30%. Analysis. Founded (%): C 45.82, H 4.91, N 3.30, Rh 23.94. Calculated for $C_{16}H_{19}NO_6Rh$: C 45.29, H 4.51, N 3.32, Rh 24.25.

Dicarbonyl(4,7-di-tert-butylbenzo[d][1,3]dithiole-2-one-5,6-dionato)rhodium (**4**).

Yield: ~40%. Analysis. Founded (%): C 43.87, H 4.28, S 14.00, Rh 21.27. Calculated for $C_{17}H_{18}O_5S_2Rh$: C 43.50, H 3.86, S 13.67, Rh 21.92.

Dicarbonyl(5,8-di-tert-butyl-2,3-dihydrobenzo[b][1,4]dioxine-6,7-dionato)rhodium (**5**).

Yield: ~40%. Analysis. Founded (%): C 49.23, H 5.25, Rh 23.00. Calculated for $C_{18}H_{22}O_6Rh$: C 49.44, H 5.07, Rh 23.53.

Dicarbonyl(5,8-di-tert-butyl-2,3-dihydro-1,4-ethanquinoxaline-6,7-dionato)rhodium (**6**).

Yield: ~70%. Analysis. Founded (%): C 51.63, H 5.50, N 6.15, Rh 23.02. Calculated for $C_{20}H_{26}N_2O_4Rh$: C 52.05, H 5.68, N 6.10, Rh 22.30.

Dicarbonyl(4,6-di-tert-butyl-N-(2,6-di-iso-propylphenyl)-o-iminobenzosemiquinonato)rhodium (**7**).

Yield: ~60%. Analysis. Founded (%): C 62.18, H 6.91, N 2.36, Rh 18.75. Calculated for $C_{28}H_{37}NO_3Rh$: C 62.44, H 6.93, N 2.61, Rh 19.11.

Acknowledgments

The authors are thankful to Russian President Grant supporting Scientific Schools (NSh-7065.2010.3), RFBR (Grants N 10-03-00788, 09-03-12241), Program of Presidium of RAS N 18, 21 and FSP "Scientific and scientific-pedagogical cadres of innovation Russia" for 2009–2013 years (GK P839 from 27.05.2010) for financial support, N.O. Druzhkov, T.N. Kocherova for quinones providing, O. Kuznetsova and N. Khamaletdinova for IR-NIR investigations.

References

[1] G.A. Razuvaev, V.K. Cherkasov, G.A. Abakumov, J. Organomet. Chem. 160 (1978) 361–371.
[2] V.I. Nevodchikov, G.A. Abakumov, V.K. Cherkasov, G.A. Razuvaev, J. Organomet. Chem. 214 (1981) 119–124.
[3] K.A. Kozhanov, M.P. Bubnov, V.K. Cherkasov, G.K. Fukin, G.A. Abakumov, Chem. Commun. 20 (2003) 2610–2611.
[4] K.A. Kozhanov, V.K. Cherkasov, G.K. Fukin, G.A. Abakumov, Dalton Trans. (2004) 2957–2962.
[5] C.W. Lange, M. Foldeaki, V.I. Nevodchikov, V.K. Cherkasov, G.A. Abakumov, C.G. Pierpont, J. Am. Chem. Soc. 114 (1992) 4220–4222.
[6] G.A. Abakumov, L.G. Abakumova, V.K. Cherkasov, V.I. Nevodchikov, Izvestiya AN SSSR (1990) 1098–1101.
[7] G.A. Abakumov, V.K. Cherkasov, T.N. Kocherova, N.O. Druzhkov, Yu.A. Kursky, M.P. Bubnov, G.K. Fukin, L.G. Abakumova, Russ. Chem. Bull. 56 (9) (2007) 1849–1856.
[8] A.I. Poddel'sky, I.V. Smolyaninov, Y.A. Kurskii, G.K. Fukin, N.T. Berberova, V.K. Cherkasov, G.A. Abakumov, J. Organomet. Chem. 695 (2010) 1215–1224.
[9] A.I. Poddel'sky, V.K. Cherkasov, M.P. Bubnov, L.G. Abakumova, G.A. Abakumov, J. Organomet. Chem. 690 (2005) 145–150.
[10] A.J. Gordon, R.A. Ford, The Chemist Companion, Wiley-Interscience, 1972.
[11] R. Colton, R.H. Farthing, J.E. Knapp, Austral. J. Chem. 23 (1970) 1351.
[12] G.A. Abakumov, V.K. Cherkasov, L.G. Abakumova, V.I. Nevodchikov, N.O. Druzhkov, N.P. Makarenko, Yu.A. Kursky, J. Organomet. Chem. 491 (1995) 127–133.
[13] G.A. Abakumov, O.N. Mamysheva, Russ. Chem. Bull. 49 (9) (2000) 1506–1511.
[14] V.A. Kuropatov, V.K. Cherkasov, Yu.A. Kursky, G.K. Fukin, L.G. Abakumova, G.A. Abakumov, Russ. Chem. Bull. Int. Ed. 55 (4) (2006) 708–711.
[15] T.I. Prokof'eva, V.B. Vol'eva, A.I. Prokof'ev, I.S. Belokhvostikova, N.L. Komisarov, V.V. Ershov, Khim. Geterocikl. Soed. 36 (8) (2000) 1057.
[16] G.A. Abakumov, N.O. Druzhkov, Yu.A. Kursky, A.S. Shavyrin, Russ. Chem. Bull. Int. Ed. 52 (2003) 712.
[17] A.I. Poddel'sky, G.A. Abakumov, M.P. Bubnov, V.K. Cherkasov, L.G. Abakumova, Russ. Chem. Bull. Int. Ed. 53 (2004) 1189.